Added value of *a priori* bias correcting dynamically downscaled data for application to species distribution models - a case study for coastal British Columbia

Dipti Hingmire[1*], Jennifer McHenry[2●], Julia Velletta[1,3●], Vanessa Valenti[4], Julia K. Baum[2]

1 School of Earth and Ocean Sciences, University of Victoria, Victoria, British Columbia, Canada, V8P 5C2
2 Department of Biology, University of Victoria, Victoria, British Columbia, Canada, V8P 5C2
3 Canadian Centre for Climate Modelling and Analysis, Environment and Climate Change Canada, Victoria, British Columbia, Canada, V8N 1V8
4 Department of Geography, The University of British Columbia, Vancouver, British Columbia, Canada, V6T 1Z4.

●These authors contributed equally to this work.
* hingmiredipti7@gmail.com

Abstract

Predicting changes in species distributions under climate change relies on high-quality climate projections. In this case study of coastal British Columbia, we prepare and evaluate two sets of climate data - *a priori* bias corrected and non bias corrected dynamically downscaled historical projections of Community Earth System Model 2 simulations. We compare these datasets with downscaled ERA5 reanalysis focusing on commonly used inputs to species distribution models (SDM), namely, bioclimatic (BIOCLIM) variables and climate extreme indices. Our results show improvements for mean BIOCLIM variables when *a priori* bias correction is applied. However, modest improvements are observed in terms of variability and extreme indices. Overall, our findings suggest that *a priori* bias corrected dynamically downscaled climate projections provide more accurate input to SDMs, and thus can improve the reliability of these important ecological models.

Introduction   1

Coastal and marine ecosystems harbor biodiversity and provide a number of important   2
ecosystem services, including fisheries production, water filtration, coastal protection,   3
and carbon storage, all of which depend on the species that inhabit these   4
ecosystems. [1–4]. There is growing evidence that these ecosystems are adversely   5
impacted by climate change along with other human stressors [4]. To study how these   6
ecosystems may change in the future, researchers and practitioners commonly employ   7
species distribution models (hereafter SDM), which predict species distribution based on   8
the relationship between species occurrence patterns and environmental variables using   9
various statistical and machine learning techniques [5]. Although SDMs are now   10
mainstream tools in ecology, biogeography, and, conservation planning and management,   11
the performance and accuracy of SDM predictions can vary widely because of their   12

strong dependance on the quality of environmental and climate data used as inputs [6–8]. Given that SDMs require high-resolution datasets, ecological modellers often use interpolated or statistically downscaled global datasets like WorldClim2 [9] or 'Climatologies at High resolution for the Earth's Land Surface Areas'(CHELSA, [10]). However, these data may differ substantially from more accurate regional downscaling efforts, potentially compromising the prediction of future species distributions [11].

The main predictors used in SDMs are climate variables, including surface temperature and precipitation, which play a major role in determining species geographic range limits and distributions in coastal ecosystems [12, 13]. In the eighties, Nix [14] defined a special set of climate indices, called bioclimatic (BIOCLIM) variables, that relate climatic conditions to species physiology. This set of 19 variables is still widely used for the development of SDMs with slight modifications [15]. BIOCLIM variables capture annual and seasonal means, ranges, and seasonality of temperature and precipitation separately and together [16, 17]. Assessing the impact of climate change on species is becoming more important for better planning of conservation and risk management.

Climate change not only shifts average climate regimes, but also exacerbates the frequency, duration, and intensity of extreme weather and climate events [18]. These mean changes and extreme event occurrences can drive species redistribution [19–21] and even extinction if suitable conditions disappear [22]. Yet, despite their importance extreme events have often been overlooked in SDM studies [23, 24]. Recently, however researchers and practitioners have called attention to this gap [25] and found ways to incorporate them in ecological modeling [26–29].

Global Earth System Models (ESMs) participating in Coupled Model Inter-Comparison Project 6 (CMIP6; [30]) are widely used to understand the future changes in large-scale climate across the globe [31]. For regional impact and policy studies, these projections are downscaled either dynamically, using a physics-based numerical model [32], or statistically, using empirical relationships between variables in historical data [33, 34]. Especially in the regions where orography plays a major role or in coastal regions, like the Pacific Northwest, mesoscale feedbacks are important and dynamical downscaling is able to impose important local-scale characteristics and refine coarse-resolution projections. [35, 36]. Regional climate models, used for dynamical downscaling, better resolve the regional features and hence are supposed to simulate more accurate projections [32]. But, inherent biases in ESMs propagate into dynamically downscaled regional projections [37, 38] making them unreliable for impact and adaptation studies. Over the years various bias correction methods have been proposed to improve climate projections [39]. In the case of dynamical downscaling, bias correction can be applied before (*a priori*) or after downscaling. *A priori* bias correction aims to reduce the biases from the original ESM before dynamical downscaling, which is found to result in better high-resolution climate projections [40, 41].

In this case study, we quantify the added value of *a priori* bias correcting a dynamically downscaled dataset over coastal British Columbia in the context of SDMs. We compare dynamically downscaled *a priori* bias corrected and non bias corrected historical projections with observed reanalysis dataset and present the added value using BIOCLIM variables and extreme indices. Our results show that *a priori* bias corrected dynamically downscaled data of mean BIOCLIM variables compare better to observations and provide more accurate input to SDMs which is expected to enable more realistic species projections.

Data and methods

Study region

The coast of British Columbia, Canada, spans a distance of almost 1000 km in a straight line, but its actual shoreline is much longer (more than 26000 km) due to a complex geography of fjords, inlets, headlands, islands, and beaches, encompassing diverse oceanographic and ecosystem features [42]. The unique combination of oceanography, geomorphology, and hydrology of coastal British Columbia or Canada's Pacific coast forms the complex and rich habitat for diverse coastal and terrestrial species. This coastal region comprises four marine bioregions, the Northern Shelf, Southern Shelf, Offshore Pacific, and Strait of Georgia, and one terrestrial ecozone, the Pacific Maritime (see Fig 1b). Each of these ecoregions is characterised by rich biodiversity with a set of unique flora and fauna, for more details, refer to [43–46]. These regions are also particularly vulnerable to the impacts of climate change due to their proximity to the Northeastern Pacific, where significant temperature increases are projected [47]. Thus it is imperative to understand the potential future ecosystem changes along coastal British Columbia which in-turn necessitates reliable high resolution climate projections for the region.

Fig 1. Map of study area showing WRF domains and different ecoregions a. WRF domains employed for downscaling. Orange dots show locations of stations used for evaluation of WRF simulations. Shading shows the orographic model elevation in meters. b. Zoomed part of coastal British Columbia (shown in red box in panel a) to show locations of four marine bioregions, i.e., Offshore Pacific (blue), Strait of Georgia (green), Southern Shelf (pink) and Northern Shelf (beige), and, a terrestrial ecozone, Pacific Maritime (outlined by purple boundary).

WRF configuration

We employed the Weather Research and Forecasting (WRF) model version 4.2.1 [48] to downscale climate projections. The domain setup included two nested domains with grid spacings of 36 and 12 km over the British Columbia coast (Fig 1a) and 38 vertical levels. WRF is a non-hydrostatic mesoscale modeling system which is extensively used for research and operational forecasting with demonstrative use cases for regional climate downscaling along the west coast of North America [49,50]. Following the guidelines from [36,51] and [52], we used the physics options listed in Table 1 to downscale climate simulations.

Table 1. List of physics options used in WRF downscaling.

Microphysics	1.5-moment 6-class Thompson microphysics scheme [53]
Cumulus	Grell–Freitas Ensemble Scheme [54]
Land surface	Noah–MP Land Surface Model [55]
Surface layer	Revised MM5 Scheme [56]
Planetary boundary layer	Yonsei University Scheme [57]
Longwave and shortwave radiation	Rapid Radiative Transfer Model for GCMs Shortwave and Longwave Schemes [58]

Spectral nudging with wavenumber 3 was applied in both directions to the outer domain (D1) for temperature, horizontal winds, geopotential, and humidity above the boundary layer to avoid internal model drift. We used a nudging coefficient 0.00005 for

humidity and 0.0003 for the remaining variables [59]. The lateral boundary conditions were updated at 6-hourly intervals and the model was initialized each year on August 1st and run through to August 31st of the following year following the method outlined in [60]. The first month from each run was discarded as a spin-up and the remaining data - from September 1st to August 31st - are stitched together across years to create a continuous time series covering the period from September 1st 1979 to August 31st 2014. Subsequent analysis was conducted over the full calendar years from 1980 to 2013.

Numerical experiments

Using the WRF setting described above, we performed three sets of numerical downscaling experiments for this case study. To validate the WRF setup, we downscaled reanalysis provided by the European Centre for Medium-Range Weather Forecasts (ECMWF) ERA5 [61], (WRF_ERA5 hereafter). We compared daily minimum temperature, maximum temperature, and precipitation from 984 stations located across the WRF domain (see Fig. 1a) to the WRF_ERA5. The quality controlled station data was obtained from Global Historical Climatology Network Daily (GHCNd) database (version 3.1) archived at National Centers for Environmental Information [62]. After validating WRF_ERA5, we considered this dataset as historical reference and used it to compute various biases.

We downscaled one ensemble member (r11i1p1f1) from the Community Earth System Model 2 (CESM2) [63] historical simulations in the CMIP6 dataset using two approaches: directly downscaling of the raw data (WRF_CESM2) and downscaling the data following *a priori* bias correction (WRF_CESM2_BC), as described below. These experiments aimed to elucidate the added value of *a priori* bias correction.

Bias correction method

Before dynamical downscaling, we employed a simple mean-state bias correction to the CESM2 dataset, which is then used as initial and boundary condition for the regional WRF simulations. Our correction followed a simple procedure similar to that used in [64]. We chose this simple mean-state bias correction to minimize drastic alterations to the model data and to avoid introducing potential dynamical inconsistencies [41, 65, 66]. We first applied a 91 days rolling mean in order to remove the high frequency variability. We decomposed each variable into two parts: mean climatology (1980-2013) and the anomaly from this climatology.

$$\text{Model} = \text{Model}_{\text{mean}} + \text{Model}_{\text{anom}}, \tag{1}$$

$$\text{ERA5} = \text{ERA5}_{\text{mean}} + \text{ERA5}_{\text{anom}}, \tag{2}$$

Then we calculated the biases as the difference between the two means.

$$\text{Bias} = \text{Model}_{\text{mean}} - \text{ERA5}_{\text{mean}}, \tag{3}$$

This bias was then subtracted from the model data to obtain the mean-state bias corrected values.

$$\text{Model}_{\text{BC}} = \text{Model} - \text{Bias} = \text{ERA5}_{\text{mean}} + \text{Model}_{\text{anom}}, \tag{4}$$

To address diurnal bias patterns we applied this procedure at an interval of 6 hours, i.e., separately for timesteps at which lateral boundary conditions are provided (at 00, 06, 12, and 18 UTC). In this way, at each grid point, we bias corrected core climate variables, namely temperature, moisture, horizontal winds, and sea surface temperature.

Calculation of added value

We calculated the climate statistics in terms of mean and variability for each set of downscaled data. Simple Added Value (AV) can be calculated by subtracting the distance between WRF_CESM2 and WRF_ERA5 from the distance between WRF_CESM2_BC and WRF_ERA5 [67]. Here we used the Root Mean Square Error (RMSE) as a distance metric. AVs calculated in this way can vary significantly from variable to variable. For better comparison of AV among variables, we normalised the absolute values by dividing with the sum of the distances as in the following equation [68].

$$\text{normalised AV} = \frac{R - R_{BC}}{R + R_{BC}} \tag{5}$$

where,

$$R = \text{RMSE}(\text{WRF\_ERA5}, \text{WRF\_CESM2})$$
$$R_{BC} = \text{RMSE}(\text{WRF\_ERA5}, \text{WRF\_CESM2\_BC})$$

Another metric we employed to quantify the overall AV is the normalized sign AV [68]. It is the percentage of grid points which shows positive AV.

$$\text{sign AV} = 100 * \frac{N_D}{N} \tag{6}$$

where,

$$N_D = \text{Number of grid points where}[\text{D} - \text{D}_{\text{BC}}] > 0$$
$$D = |\text{WRF\_CESM2} - \text{WRF\_ERA5}|$$
$$D_{BC} = |\text{WRF\_CESM2\_BC} - \text{WRF\_ERA5}|$$
$$N = \text{Total number of grid points}$$

Details about BIOCLIM variables and extreme indices used in this study are given in S1 Table and S2 Table respectively. Please note we analysed three additional biologically relevent variables along with the standard BIOCLIM variables; also described in S1 Table. We used python library named xclim to calculate these variables from standard climate variables [69]. Finally, we calculated the normalised AV and sign AV for all the BIOCLIM variables and extreme indices for the entire domain D2 as well as the four marine ecoregions and a terrestrial coastal ecozone along the British Columbia coast (see section Study region, Fig 1b).

Results

Evaluation of WRF_ERA5

The Fig. 2 depicts the evaluation of WRF_ERA5 against the GHCNd station observations over the study domain for years 1980-2013. We used bilinear interpolation to get WRF data at the station location. Panels a to c of Fig. 2 show the scatter plots of observed and WRF_ERA5 daily minimum temperature for the whole year as well as

summer and winter seasons respectively. WRF_ERA5 minimum temperature is positively biased with a mean warm bias of 1.49°C for the summer season and negatively biased for the winter with a mean cold bias of -0.48°C. On the other hand, maximum temperature by WRF_ERA5 shows a consistent cold bias for the whole year as well as both the seasons (Panels d-f of Fig. 2). WRF_ERA5 simulated daily precipitation shows good agreement with station observations as illustrated by the density histograms in panels g-i of Fig. 2. WRF_ERA5 simulates wet annual (0.16 mm/day) bias with summer bias (0.40 mm/day) larger than winter bias (0.07 mm/day).

Fig 2. Comparison of WRF_ERA5 with station observations. Scatter plot of WRF_ERA5 and observed station daily minimum temperature a. Annual b. JJA and c. DJF. Observed daily maximum temperature plotted against WRF_ERA5 d. Annual e. JJA and f. DJF. Density histograms of g. Annual h. JJA and i. DJF precipitation of WRF_ERA5 (blue) and observed at stations (green). All the panels show data for years 1980-2013.

To further understand the spatial distribution of these errors, we plotted annual RMSE, Pearson Correlation Coefficient (CC) and bias at each station as shown in Fig. 3. Most of the stations have RMSE of less than 2°C for minimum and maximum temperatures (Fig. 3 a,d) and less than 4 mm/day for precipitation (Fig. 3 g) but some stations show larger RMSEs for precipitation in coastal regions. The same is reflected in CC; more than 0.8 CC is observed at most of the stations for maximum and minimum temperature values but for precipitation CC range between 0.2 to 0.8 (Fig. 3 b,e,h). In terms of bias (Fig. 3 c, f, i) precipitation shows a scattered pattern with a mix of relatively small wet and dry biases. Minimum temperature has a tendency towards cold biases for northern stations and warm biases for southern stations, whereas maximum temperature shows an overall cold bias. Temperature biases appear smaller in coastal regions as opposed to inlands. Overall most of the time WRF_ERA5 values show reasonable agreement with observations. In the next section we compare the downscaled historical climate simulations with WRF_ERA5.

Fig 3. Evaluation of WRF_ERA5 using station observations. (a, d, g) RMSE, (b, e, h) Pearson correlation coefficient and (c, f, i) bias of WRF_ERA5 with observed values at each station for (a-c) minimum temperature (d -f) maximum temperature and (g-i) precipitation.

Evaluation of climatology biases

In this section we analyse the biases of the CESM2 input data and of the two downscaled experiments. CESM2 data has an original nominal horizontal resolution of 1° and is interpolated to the WRF_ERA5 grid using bilinear interpolation to calculate temperature and precipitation biases. The spatial distribution of climatological mean temperature in Fig. 4a shows clearly the expected south-to-north and elevation gradient with lower temperatures at higher latitudes and elevations. Panels b to d of Fig. 4 show the bias of CESM2, WRF_CESM2 and WRF_CESM2_BC with WRF_ERA5. CESM2 exhibits a warm bias over most of the region with a pronounced positive bias over mountain regions ranging between 4 to 6 °C (Fig. 4 b) which can be attributed to the differences in model terrain resolution between CESM2 and WRF. CESM2 shows positive bias over the oceanic region as well, with warmer bias over the northwest corner of the domain. Dynamically downscaled CESM2, i.e., WRF_CESM2, utilizes the same model terrain as WRF_ERA5 and hence shows reduction in biases over most of the land region. However, the oceanic bias remains the same (Fig. 4 c) indicating persistence of

systematic bias of CESM2 in downscaled product. *A priori* bias correction applied to WRF_CESM2_BC is further able to significantly reduce the biases present in WRF_CESM2 as shown in Fig. 4 d.

Fig 4. Climatology and bias in daily mean climatology of temperature and precipitation. Spatial distribution of daily mean climatology of WRF_ERA5 a. air temperature and e. precipitation. Biases of daily mean (b-d) air temperature and (f-h) precipitation for (b,f) CESM2 (c,g) WRF_CESM2 and (d,h) WRF_CESM2_BC. Please note that scale used for CESM2 bias (b) uses a wider range of values than WRF_CESM2 (c) and WRF_CESM2_BC (d) for the same color palette to depict higher biases.

The spatial distribution of climatological mean precipitation of WRF_ERA5 (Fig. 4 e) exhibits the orographic peak precipitation over the mountainous region along the coast, Haida Gwaii archipelago, and Vancouver Island. Due to low resolution, CESM2 cannot resolve the true orography and shows large dry bias over these regions (Fig. 4 f). WRF_CESM2 resolves most of these smaller-scale topographic biases (Fig. 4 g) but some widespread biases persist. WRF_CESM2_BC shows further improvements (Fig. 4 h); although it exhibits slight dry bias along the Coast mountains, biases are reduced to below ±1 mm/day across the domain. We also considered the mean of daily minimum temperature, maximum temperature and maximum 5-day and 10-day accumulated precipitation (S1 Fig and S2 Fig). For these quantities as well WRF_CESM2_BC alleviates the biases present in WRF_CESM2. In short, WRF_CESM2_BC represents historical mean climatologies better than WRF_CESM2. In the following we will explore how these improvements in mean translate into added value for BIOCLIM and extreme indices.

Added value of *a priori* bias correction - BIOCLIM variables

Fig. 5 a and b shows the normalised and sign AV for mean BIOCLIM variables over the entire domain and five ecoregions of coastal British Columbia. Majority of BIOCLIM variables show positive normalised AV and more than 50% sign AV, demonstrating benefits of *a priori* bias correction. Improvements seen are not uniform across different regions. The Strait of Georgia, Southern Shelf marine bioregion and Pacific Maritime terrestrial ecozone show positive normalised values for the highest number of BIOCLIM variables (17 out of 22 in each region), while the Northern Shelf bioregion sees improvement with positive normalised AV for the smallest total number of BIOCLIM variables, which is still 13 out of 22 variables.

In terms of variables, isothermality has the highest number of negative normalised AVs. On the other hand, 8 variables, namely, annual mean temperature, annual mean diurnal range, minimum temperature of coldest month, mean temperature of wettest quarter, precipitation of driest month, precipitation of wettest quarter, heating degree days and growing degree days, showed improvements over all the regions in terms of normalised AV.

Fig 5. Added value for mean BIOCLIM variables. a. Normalised AV and b. Sign AV for climatological mean of WRF_CESM2_BC over WRF_CESM2 for various BIOCLIM indices over different ecoregions.

Sign AV shown in Fig. 5 b expresses similar results, where most of the time positive normalised AV also has more than 50% value for sign AV. But sometimes even though normalised AV is positive less than 50% of the grid points show improvements. For example, the normalised AV value for precipitation of wettest quarter over the whole, i.e., All domain, is 0.26 but the sign AV is only 36.1% meaning few points show large

improvements but many other points don't. We also observe cases where modest positive value of normalised AV corresponds to 100% sign AV, implying incremental improvements are spatially spread, e.g., case of mean temperature of wettest quarter for Strait of Georgia. The charts of the sign AV and normalised AV in Fig. 5, illustrate that WRF_CESM2_BC provides better climatological means of BIOCLIM variables than WRF_CESM2. S3 Fig is similar to Fig. 5 but depicts variability, i.e., interannual standard deviation of BIOCLIM variables. Contrary to the case of mean, the variability of BIOCLIM variables shows no or slight added value from bias correction by WRF_CESM2_BC which is likely due to the nature of simple bias correction, that is focused on correcting the mean state and not the variability of climate simulation.

Added value of *a priori* bias correction - extreme indices

We further examined the AVs for extreme temperature and precipitation indices depicted in Fig. 6. Most of the indices show positive normalised AV value (Fig. 6 a) but this is not reflected in the sign AV chart (Fig. 6 b). Dry and wet spell indices perform better than hot and cold spell indices (Fig. 6 b) over many regions except the Pacific Maritime ecozone. For the wet spell frequency index all the regions showed positive normalised AV and more than 50% sign AV. Inconsistency between normalised AV and sign AV is conspicuous in case of hot and cold spell indices for the northern shelf bioregion as well as All domain and can likely be explained by the few locations with large added value but larger areas of slightly reduced AV. S4 Fig shows similar AV charts for variability of extreme indices. Akin to BIOCLIM variables, extreme indices also show no or negligible improvements from bias correction in terms of standard deviation. Mean BIOCLIM variables show clear ameriolations because of *a priori* bias correction in WRF_CESM2_BC, but the extreme indices show mixed signals depending on variable and region.

Fig 6. Added value for mean extreme indices. a. Normalised AV and b. Sign AV for climatological mean of WRF_CESM2_BC over WRF_CESM2 for various extreme indices over different ecoregions.

In summary, *a priori* bias correction applied in WRF_CESM2_BC produces better climate simulation with improvements in mean climatologies of standard variables like temperature, precipitation and the BIOCLIM variables. On the other hand little to no added value is observed for mean climatology of extreme indices as well as standard deviation of all the variables.

Discussion

In this case study, we examined the value of *a priori* bias correcting dynamically downscaled data for application to ecological SDMs. Specifically, we compared downscaled reanalysis with downscaled historical simulations of an ensemble member of CESM2 over coastal British Columbia. For mean climatologies of standard variables like temperature, precipitation and biologically relevant BIOCLIM indices, we showed that *a priori* bias corrected downscaled projections are better than non bias corrected counterparts. Most BIOCLIM indices showed an overall positive added value of *a priori* bias correction, with improvements observed in majority of the grid points across all ecoregions. Although the benefits of *a priori* bias correction have been known for more than a decade [64], this has only recently been used to generate datasets [41,70]. These studies mainly discussed benefits in terms of basic climate variables and processes,

whereas in this study, we show improvements for a variety of ecologically relevant variables.

Improvements in mean climate variables from *a priori* bias correction, as shown in this study, have important implications for ecological modeling in regions like coastal British Columbia, where complex topography and coastal geomorphology interact to create microclimates that differ from broader climate trends [71]. Many marine and terrestrial species in coastal environments have sharp physiological thresholds for temperature and moisture [72–75], which are likely to be better captured by high-resolution, *a priori* bias corrected datasets. Improved representation of local climate conditions is expected to lead to more realistic SDM predictions, especially in fjords, narrow inlets, or island archipelagos where coarse datasets often miss key environmental gradients. This spatial precision may be particularly valuable for identifying potential climate refugia and priority areas for climate-smart conservation strategies [76].

Although *a priori* bias correction has improved the mean of BIOCLIM variables, we found marginal improvements for the mean of extreme indices and interannual variability; which is likely due to the simple mean bias correction technique that we utilize. We surmise that more sophisticated bias correction techniques like quantile mapping could improve the interannual variability [77]. However, when selecting the bias correction method, it is important to avoid introducing inconsistencies among input variables used for downscaling. Improvements in extreme indices could be achieved by mean-variance-trend bias correction [78] as shown in [79].

While our study demonstrates the added value of *a priori* bias correction using a single ensemble member from one ESM, it would be valuable to extend this proof of concept to a broader range of models. Given that most ESMs exhibit some degree of systemic bias, we hypothesize that *a priori* bias correction could be beneficial across models. However, the extent of improvement will likely vary depending on the magnitude and characteristics of each model's inherent bias. For instance, models with pronounced diurnal bias patterns might benefit from time-of-day dependent bias correction; however, our study showed marginal improvement from such considerations using CESM2. Ideally, some analysis of ESM outputs should be carried out before deciding on a bias correction method. When downscaling future climate projections, it is common to use large ensembles of different climate models and multiple scenarios to assess uncertainty. To limit the computational cost of dynamical downscaling in ensemble applications, after bias correcting the coarse-resolution inputs, novel approaches have been developed that combine dynamical downscaling with generative AI to efficiently estimate uncertainty bounds of downscaled climate projections [80].

High-quality input data are a critical component of SDMs and warrant careful consideration during selection. Seo et al. [81] showed that coarse resolution climate projections impair the quality of biological SDM outputs whereas Fortini et al. [11] demonstrated that statistically downscaled climate data also possess some problems like difficulties in replicating local fine-scale temperature and precipitation patterns and large uncertainty between datasets based on method used for downscaling. Therefore, many researchers advocate for dynamical downscaling, while recognizing that dynamically downscaled data can also retain certain flaws, such as preserving original ESM biases. However, our study for coastal British Columbia demonstrates that *a priori* bias correction can effectively address these biases.

In practice, the choice of climate inputs for SDMs often involves a trade-off between data quality and feasibility. For ecologists working in topographically complex regions or focusing on species with narrow environmental tolerances, investing in high-resolution, bias-corrected data may be critical for accurately capturing species' current distributions, range edges, and fine-scale distributional shifts. Especially in

heterogeneous landscapes and climate sensitive environments, we encourage ecologists and conservation practitioners to seek collaborations with atmospheric scientists and regional climate modelers to access or co-develop tailored downscaled datasets. These interdisciplinary partnerships can help bridge the gap between climate modeling and ecological application.

Given resource constraints and limited climate modelling expertise among ecologists, comprehensive bias correction and dynamical downscaling are not always feasible. In such cases, when practitioners rely on statistical downscaling or directly use ESM output as inputs to SDMs, we recommend carefully selecting the ESM considering its inherent biases and errors and clearly communicating them to stakeholders. However, where possible, our findings suggest that *a priori* bias corrected dynamically downscaled data can serve as better input to SDMs for more reliable predictions. Overall, to advance the use of more accurate inputs to SDMs in future, we recommend fostering interdisciplinary collaborations between physical climate scientists and ecologists, to ensure the best possible data are used.

Supporting information

S1 Fig.   Climatology and biases of minimum and maximum temperature Spatial distribution of daily mean climatology of WRF_ERA5 a. minimum air temperature and d. maximum air temperature. Biases of daily mean (b,c) minimum air temperature and (e,f) maximum air temperature for (b,e) WRF_CESM2 and (c,f) WRF_CESM2_BC.

S2 Fig.   Climatology and biases of 5-day and 10-day maximum precipitation. Spatial distribution of climatology of WRF_ERA5 a. 5-day maximum precipitation and d. 10-day maximum precipitation. Biases of mean (b,c) 5-day maximum precipitation and (e,f) 10-day maximum precipitation for (b,e) WRF_CESM2 and (c,f) WRF_CESM2_BC.

S3 Fig.   Added value for variability of BIOCLIM variables. a. Normalised AV and b. Sign AV for interannual standard deviation of WRF_CESM2_BC over WRF_CESM2 for various BIOCLIM variables over different ecoregions.

S4 Fig.   Added value for variability of extreme indices. a. Normalised AV and b. Sign AV for interannual standard deviation of WRF_CESM2_BC over WRF_CESM2 for various extreme indices over different ecoregions.

S1 Table.   BIOCLIM variables. Details about BIOCLIM variables used in this study.

S2 Table.   Extreme indices. Details about extreme indices used in this study.

Acknowledgments

the fruitful discussions, in shaping the study, with Manpreet Kaur, Timothy Chui, Graham Epstein and Mathew Csordas.

References

1. Barbier EB, Hacker SD, Kennedy C, Koch EW, Stier AC, Silliman BR. The value of estuarine and coastal ecosystem services. Ecological monographs. 2011;81(2):169–193.

2. Singh GG, Eddy IM, Halpern BS, Neslo R, Satterfield T, Chan KM. Mapping cumulative impacts to coastal ecosystem services in British Columbia. PloS one. 2020;15(5):e0220092.

3. Filbee-Dexter K, Wernberg T, Barreiro R, Coleman MA, de Bettignies T, Feehan CJ, et al. Leveraging the blue economy to transform marine forest restoration. Journal of Phycology. 2022;58(2):198–207.

4. Wernberg T, Thomsen MS, Baum JK, Bishop MJ, Bruno JF, Coleman MA, et al. Impacts of climate change on marine foundation species. Annual review of marine science. 2024;16(1):247–282.

5. Guisan A, Thuiller W, Zimmermann NE. Habitat suitability and distribution models: with applications in R. Cambridge University Press; 2017.

6. Jimenez-Valverde A, Rodriguez-Rey M, Pena-Aguilera P. Climate data source matters in species distribution modelling: the case of the Iberian Peninsula. Biodiversity and Conservation. 2021;30(1):67–84.

7. Abdulwahab UA, Hammill E, Hawkins CP. Choice of climate data affects the performance and interpretation of species distribution models. Ecological Modelling. 2022;471:110042.

8. Rodríguez-Rey M, Jiménez-Valverde A. Differing sensitivity of species distribution modelling algorithms to climate data source. Ecological Informatics. 2024;79:102387.

9. Fick SE, Hijmans RJ. WorldClim 2: new 1-km spatial resolution climate surfaces for global land areas. International journal of climatology. 2017;37(12):4302–4315.

10. Karger DN, Conrad O, Böhner J, Kawohl T, Kreft H, Soria-Auza RW, et al. Climatologies at high resolution for the earth's land surface areas. Scientific data. 2017;4(1):1–20.

11. Berio Fortini L, Kaiser LR, Frazier AG, Giambelluca TW. Examining current bias and future projection consistency of globally downscaled climate projections commonly used in climate impact studies. Climatic Change. 2023;176(12):169.

12. Guisan A, Zimmermann NE. Predictive habitat distribution models in ecology. Ecological modelling. 2000;135(2-3):147–186.

13. Amiri M, Tarkesh M, Jafari R, Jetschke G. Bioclimatic variables from precipitation and temperature records vs. remote sensing-based bioclimatic variables: Which side can perform better in species distribution modeling? Ecological informatics. 2020;57:101060.
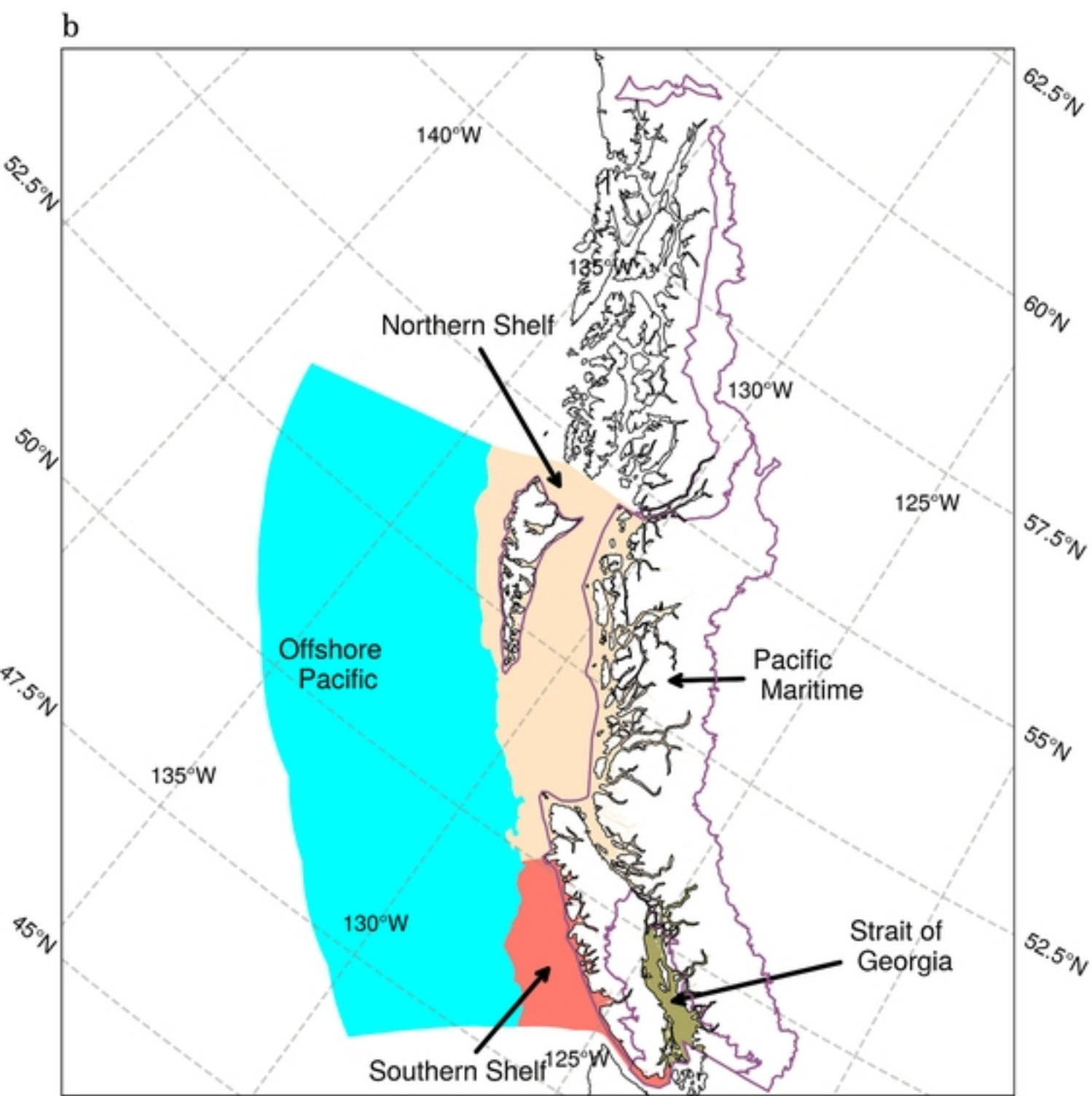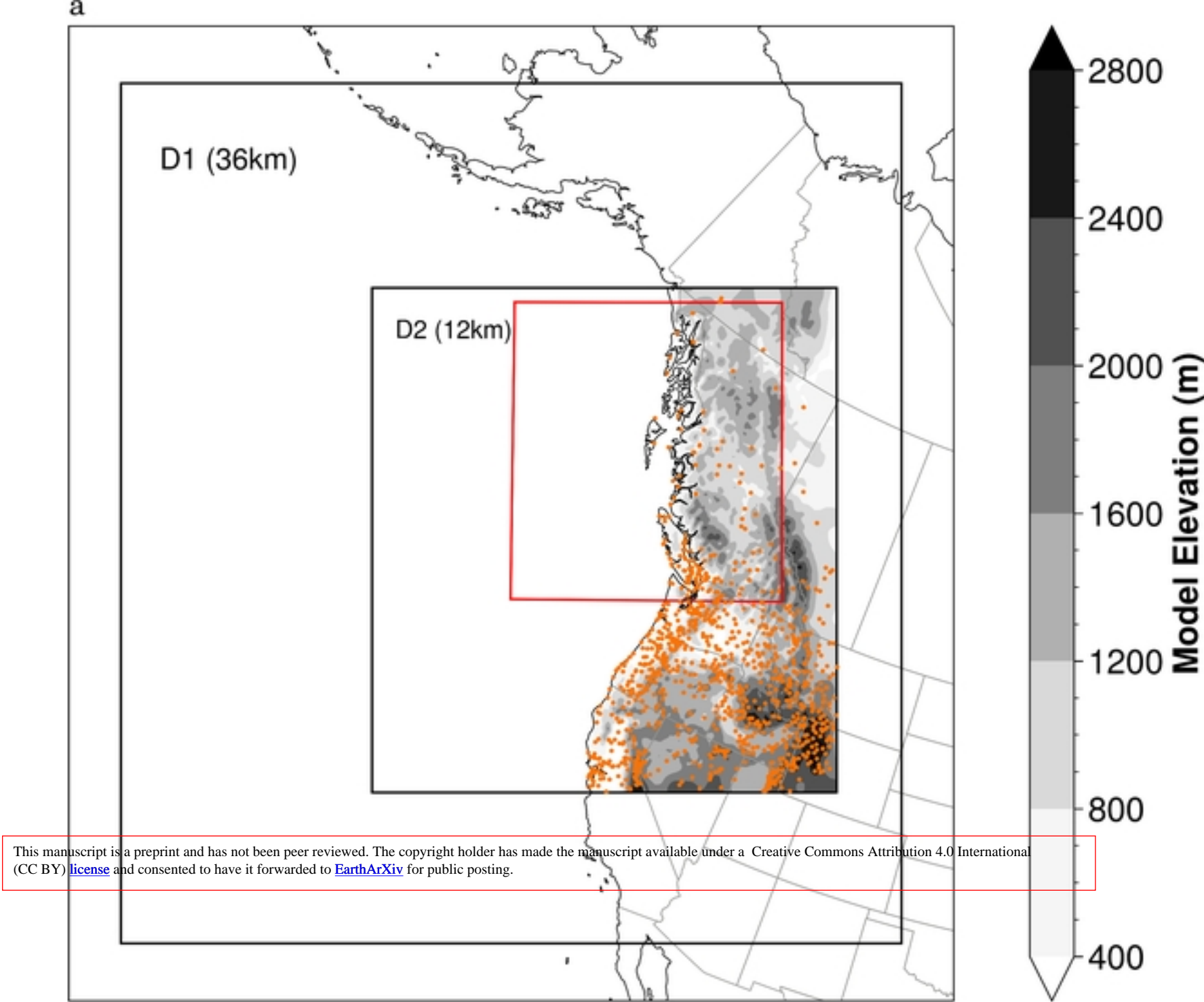
14. Nix H. A biogeographic analysis of Australian elapid snakes in RC Longmore (ed). Atlas of Australian elapid snakes. Australian Flora and Fauna Series No. 7: 4-15; 1986.

15. Bradie J, Leung B. A quantitative synthesis of the importance of variables used in MaxEnt species distribution models. Journal of Biogeography. 2017;44(6):1344–1361.

16. O'Donnel MS, Ignizio DA. Bioclimatic predictors for supporting ecological applications in the conterminous United States. US Geological Survey; 2012.

17. Booth TH. Why understanding the pioneering and continuing contributions of BIOCLIM to species distribution modelling is important. Austral ecology. 2018;43(8):852–860.

18. Seneviratne SI, Zhang X, Adnan M, Badi W, Dereczynski C, Luca AD, et al. Weather and climate extreme events in a changing climate. 2021;.

19. Briscoe NJ, Kearney MR, Taylor CA, Wintle BA. Unpacking the mechanisms captured by a correlative species distribution model to improve predictions of climate refugia. Global Change Biology. 2016;22(7):2425–2439.

20. Wernberg T, Bennett S, Babcock RC, De Bettignies T, Cure K, Depczynski M, et al. Climate-driven regime shift of a temperate marine ecosystem. Science. 2016;353(6295):169–172.

21. Seabrook L, McAlpine C, Rhodes J, Baxter G, Bradley A, Lunney D. Determining range edges: habitat quality, climate or climate extremes? Diversity and Distributions. 2014;20(1):95–106.

22. Mitchell PJ, O'Grady AP, Hayes KR, Pinkard EA. Exposure of trees to drought-induced die-off is defined by a common climatic threshold across different vegetation types. Ecology and Evolution. 2014;4(7):1088–1101.

23. Jentsch A, Kreyling J, Beierkuhnlein C. A new generation of climate-change experiments: events, not trends. Frontiers in Ecology and the Environment. 2007;5(7):365–374.

24. Ummenhofer CC, Meehl GA. Extreme weather and climate events with ecological relevance: a review. Philosophical Transactions of the Royal Society B: Biological Sciences. 2017;372(1723):20160135.

25. Soifer LG, Lockwood JL, Lembrechts JJ, Antão LH, Klinges D, Senior RA, et al. Why extreme events matter for species redistribution. 2025;.

26. Germain SJ, Lutz JA. Climate extremes may be more important than climate means when predicting species range shifts. Climatic Change. 2020;163(1):579–598.

27. Perez-Navarro MA, Broennimann O, Esteve MA, Bagaria G, Guisan A, Lloret F. Comparing climatic suitability and niche distances to explain populations responses to extreme climatic events. Ecography. 2022;2022(11):e06263.

28. Dobson R, Willis SG, Jennings S, Cheke RA, Challinor AJ, Dallimer M. Near-Term Forecasting of Terrestrial Mobile Species Distributions for Adaptive Management Under Extreme Weather Events. Global Change Biology. 2024;30(11):e17579.

29. Fonteyn W, Serra-Diaz JM, Muys B, Van Meerbeek K. Incorporating climatic extremes using the GEV distribution improves SDM range edge performance. Journal of Biogeography. 2025;52(3):780–791.

30. Eyring V, Bony S, Meehl GA, Senior CA, Stevens B, Stouffer RJ, et al. Overview of the Coupled Model Intercomparison Project Phase 6 (CMIP6) experimental design and organization. Geoscientific Model Development. 2016;9(5):1937–1958.

31. Bush E. Canada's changing climate report in light of the latest global science assessment. Government of Canada= Gouvernement du Canada; 2022.

32. Giorgi F. Thirty years of regional climate modeling: where are we and where are we going next? Journal of Geophysical Research: Atmospheres. 2019;124(11):5696–5723.

33. Wilby RL, Wigley TM. Downscaling general circulation model output: a review of methods and limitations. Progress in physical geography. 1997;21(4):530–548.

34. Kotamarthi R, Hayhoe K, Wuebbles D, Mearns LO, Jacobs J, Jurado J. Downscaling techniques for high-resolution climate projections: From global change to local impacts. Cambridge University Press; 2021.

35. Walton D, Berg N, Pierce D, Maurer E, Hall A, Lin YH, et al. Understanding differences in California climate projections produced by dynamical and statistical downscaling. Journal of Geophysical Research: Atmospheres. 2020;125(19):e2020JD032812.

36. Mass CF, Salathé Jr EP, Steed R, Baars J. The mesoscale response to global warming over the Pacific Northwest evaluated using a regional climate model ensemble. Journal of Climate. 2022;35(6):2035–2053.

37. Liang XZ, Kunkel KE, Meehl GA, Jones RG, Wang JX. Regional climate models downscaling analysis of general circulation models present climate biases propagation into future change projections. Geophysical research letters. 2008;35(8).

38. Rocheta E, Evans JP, Sharma A. Correcting lateral boundary biases in regional climate modelling: the effect of the relaxation zone. Climate Dynamics. 2020;55(9):2511–2521.

39. Dinh TLA, Aires F. Revisiting the bias correction of climate models for impact studies. Climatic Change. 2023;176(10):140.

40. Risser MD, Rahimi S, Goldenson N, Hall A, Lebo ZJ, Feldman DR. Is bias correction in dynamical downscaling defensible? Geophysical Research Letters. 2024;51(10):e2023GL105979.

41. Rahimi S, Huang L, Norris J, Hall A, Goldenson N, Risser M, et al. Understanding the cascade: Removing GCM biases improves dynamically downscaled climate projections. Geophysical Research Letters. 2024;51(9):e2023GL106264.

42. Starko S, Timmer B, Reshitnyk L, Csordas M, McHenry J, Schroeder S, et al. Local and regional variation in kelp loss and stability across coastal British Columbia. Marine Ecology Progress Series. 2024;733:1–26.
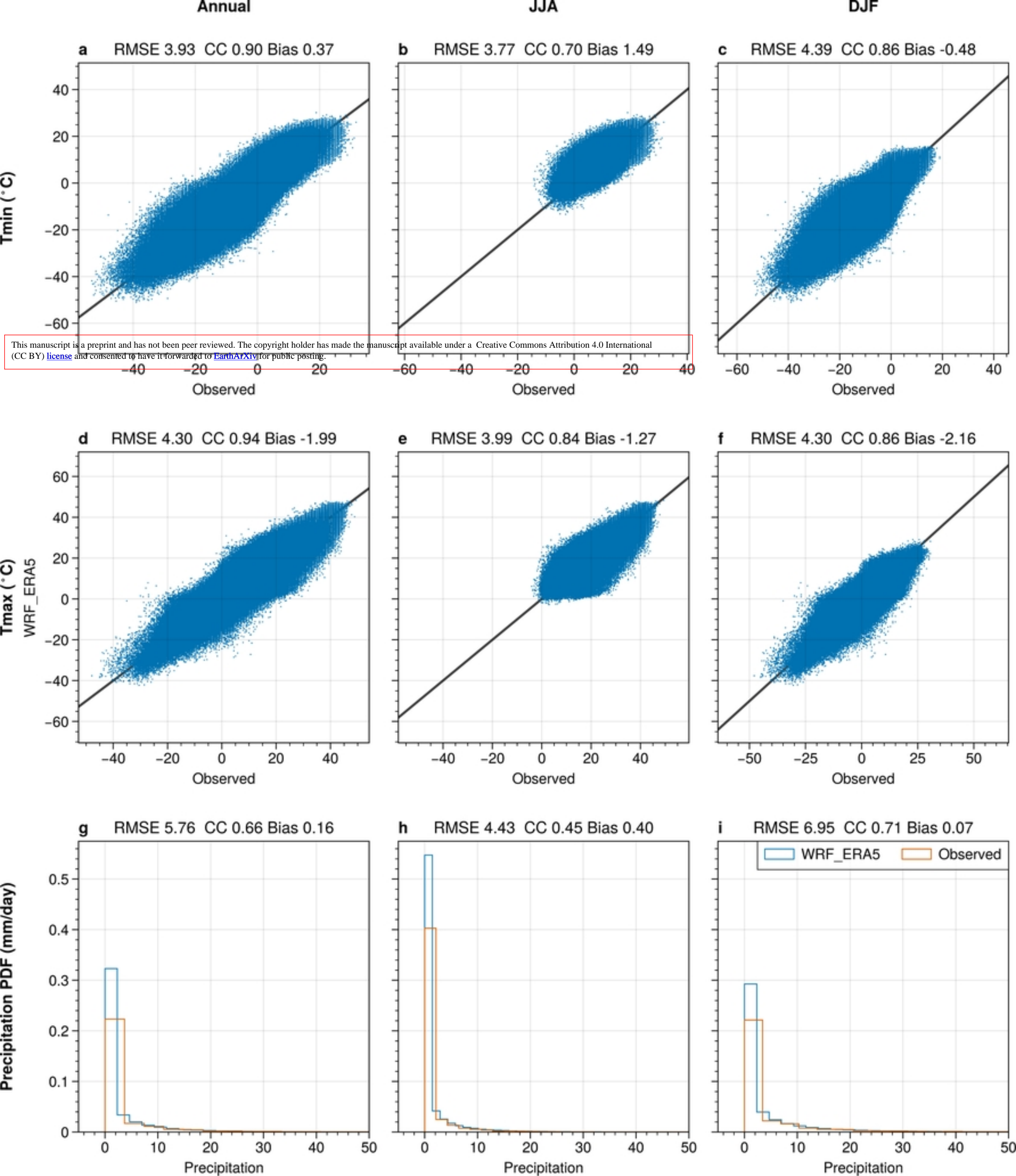
43. Department of Fisheries and Oceans. Development of a framework and principles for the biogeographic classification of Canadian marine areas. Canadian Science Advisory Secretariat Science Advisory Report 2009/056. 2009;.

44. Rubidge E, Gale KS, Curtis JM, McClelland E, Feyrer L, Bodtker K, et al. Methodology of the pacific marine ecological classification system and its application to the Northern and Southern Shelf Bioregions. Canadian Science Advisory Secretariat (CSAS); 2016.

45. Wiken EB. Terrestrial ecozones of Canada. Environment Canada, Lands Directorate Ottawa; 1986.

46. Demarchi DA. An introduction to the ecoregions of British Columbia. Ecosystem Information Section, Ministry of Environment, Victoria, British Columbia; 1996.

47. Okey TA, Alidina HM, Lo V, Jessen S. Effects of climate change on Canada's Pacific marine ecosystems: a summary of scientific knowledge. Reviews in Fish Biology and Fisheries. 2014;24(2):519–559.

48. Skamarock WC, Klemp JB, Dudhia J, Gill DO, Liu Z, Berner J, et al. A description of the advanced research WRF version 4. NCAR; 2019. TN-556+STR.

49. Jeworrek J, West G, Stull R. Optimizing analog ensembles for sub-daily precipitation forecasts. Atmosphere. 2022;13(10):1662.

50. Salathé Jr EP, Beggs A, McJunkin C, Sandhu S. The relative warming rates of heat events and median days in the Pacific Northwest from observations and a regional climate model. Journal of Climate. 2023;36(8):2471–2481.

51. Jeworrek J, West G, Stull R. Evaluation of cumulus and microphysics parameterizations in WRF across the convective gray zone. Weather and Forecasting. 2019;34(4):1097–1115.

52. Jeworrek J, West G, Stull R. WRF precipitation performance and predictability for systematically varied parameterizations over complex terrain. Weather and Forecasting. 2021;36(3):893–913.

53. Thompson G, Field PR, Rasmussen RM, Hall WD. Explicit forecasts of winter precipitation using an improved bulk microphysics scheme. Part II: Implementation of a new snow parameterization. Monthly weather review. 2008;136(12):5095–5115.

54. Grell GA, Freitas SR. A scale and aerosol aware stochastic convective parameterization for weather and air quality modeling. Atmospheric Chemistry and Physics. 2014;14(10):5233–5250.

55. Niu GY, Yang ZL, Mitchell KE, Chen F, Ek MB, Barlage M, et al. The community Noah land surface model with multiparameterization options (Noah-MP): 1. Model description and evaluation with local-scale measurements. Journal of Geophysical Research: Atmospheres. 2011;116(D12).

56. Jiménez PA, Dudhia J. Improving the representation of resolved and unresolved topographic effects on surface wind in the WRF model. Journal of Applied Meteorology and Climatology. 2012;51(2):300–316.

57. Hong SY, Noh Y, Dudhia J. A new vertical diffusion package with an explicit treatment of entrainment processes. Monthly weather review. 2006;134(9):2318–2341.

58. Iacono MJ, Delamere JS, Mlawer EJ, Shephard MW, Clough SA, Collins WD. Radiative forcing by long-lived greenhouse gases: Calculations with the AER radiative transfer models. Journal of Geophysical Research: Atmospheres. 2008;113(D13).

59. Spero TL, Nolte CG, Mallard MS, Bowden JH. A maieutic exploration of nudging strategies for regional climate applications using the WRF model. Journal of Applied Meteorology and Climatology. 2018;57(8):1883–1906.

60. Rahimi S, Krantz W, Lin YH, Bass B, Goldenson N, Hall A, et al. Evaluation of a reanalysis-driven configuration of WRF4 over the western United States from 1980 to 2020. Journal of Geophysical Research: Atmospheres. 2022;127(4):e2021JD035699.

61. Hersbach H, Bell B, Berrisford P, Hirahara S, Horányi A, Muñoz-Sabater J, et al. The ERA5 global reanalysis. Quarterly journal of the royal meteorological society. 2020;146(730):1999–2049.

62. Menne MJ, Durre I, Vose RS, Gleason BE, Houston TG. An overview of the global historical climatology network-daily database. Journal of atmospheric and oceanic technology. 2012;29(7):897–910.

63. Danabasoglu G, Lamarque JF, Bacmeister J, Bailey D, DuVivier A, Edwards J, et al. The community earth system model version 2 (CESM2). Journal of Advances in Modeling Earth Systems. 2020;12(2):e2019MS001916.

64. Bruyère CL, Done JM, Holland GJ, Fredrick S. Bias corrections of global models for regional climate simulations of high-impact weather. Climate Dynamics. 2014;43(7):1847–1856.

65. Maraun D, Shepherd TG, Widmann M, Zappa G, Walton D, Gutiérrez JM, et al. Towards process-informed bias correction of climate change simulations. Nature Climate Change. 2017;7(11):764–773.

66. Iturbide M, Casanueva A, Bedia J, Herrera S, Milovac J, Gutiérrez JM. On the need of bias adjustment for more plausible climate change projections of extreme heat. Atmospheric Science Letters. 2022;23(2):e1072.

67. Di Luca A, de Elía R, Laprise R. Challenges in the quest for added value of regional climate dynamical downscaling. Current Climate Change Reports. 2015;1(1):10–21.

68. Di Luca A, Argüeso D, Evans JP, De Elía R, Laprise R. Quantifying the overall added value of dynamical downscaling and the contribution from different spatial scales. Journal of Geophysical Research: Atmospheres. 2016;121(4):1575–1590.

69. Bourgault P, Huard D, Smith TJ, Logan T, Aoun A, Lavoie J, et al. xclim: xarray-based climate data analytics. Journal of Open Source Software. 2023;8(85):5415.

70. Kim Y, Evans JP, Sharma A. Correcting Multivariate Biases in Regional Climate Model Boundaries: How Are Synoptic Systems Impacted Over the Australian Region? Geophysical Research Letters. 2024;51(21):e2024GL111445.

71. Bramer I, Anderson BJ, Bennie J, Bladon AJ, De Frenne P, Hemming D, et al. Advances in monitoring and modelling climate at ecologically relevant scales. In: Advances in ecological research. vol. 58. Elsevier; 2018. p. 101–161.
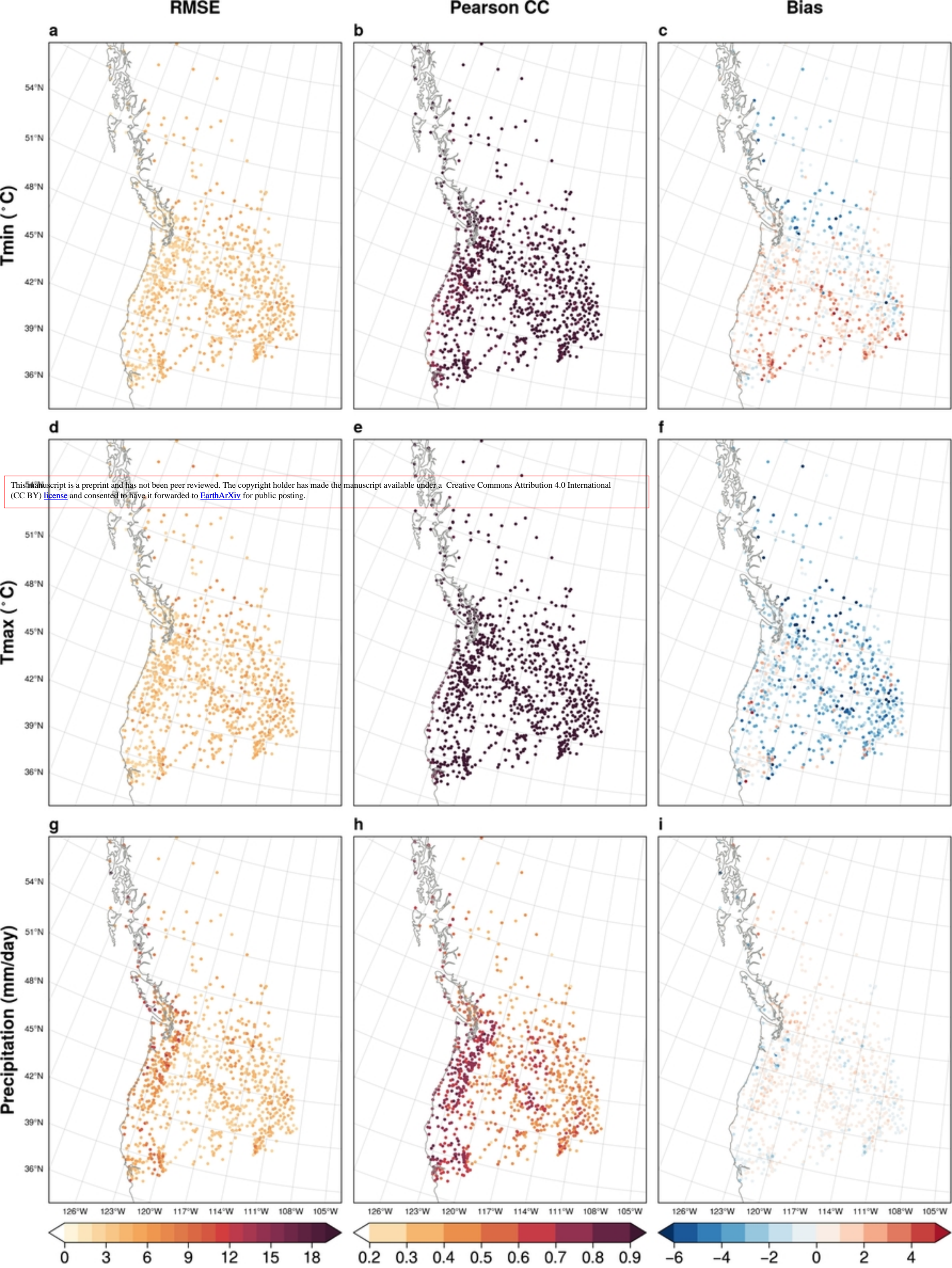
72. Pörtner HO. Climate variations and the physiological basis of temperature dependent biogeography: systemic to molecular hierarchy of thermal tolerance in animals. Comparative Biochemistry and Physiology Part A: Molecular & Integrative Physiology. 2002;132(4):739–761.

73. Sunday JM, Bates AE, Dulvy NK. Global analysis of thermal tolerance and latitude in ectotherms. Proceedings of the Royal Society B: Biological Sciences. 2011;278(1713):1823–1830.

74. Bennett JM, Calosi P, Clusella-Trullas S, Martínez B, Sunday J, Algar AC, et al. GlobTherm, a global database on thermal tolerances for aquatic and terrestrial organisms. Scientific Data. 2018;5(1):1–7.

75. Marbà N, Jordà G, Bennett S, Duarte CM. Seagrass thermal limits and vulnerability to future warming. Frontiers in Marine Science. 2022;9:860826.

76. Morelli TL, Daly C, Dobrowski SZ, Dulen DM, Ebersole JL, Jackson ST, et al. Managing climate change refugia for climate adaptation. PloS one. 2016;11(8):e0159909.

77. Cannon AJ. Multivariate quantile mapping bias correction: an N-dimensional probability density function transform for climate model simulations of multiple variables. Climate dynamics. 2018;50(1):31–49.

78. Xu Z, Han Y, Tam CY, Yang ZL, Fu C. Bias-corrected CMIP6 global dataset for dynamical downscaling of the historical and future climate (1979–2100). Scientific Data. 2021;8(1):293.

79. Zhang MZ, Han Y, Xu Z, Guo W. Assessing climate extremes in dynamical downscaling simulations driven by a novel bias-corrected CMIP6 data. Journal of Geophysical Research: Atmospheres. 2024;129(18):e2024JD041253.

80. Lopez-Gomez I, Wan ZY, Zepeda-Núñez L, Schneider T, Anderson J, Sha F. Dynamical-generative downscaling of climate model ensembles. Proceedings of the National Academy of Sciences. 2025;122(17):e2420288122.

81. Seo C, Thorne JH, Hannah L, Thuiller W. Scale effects in species distribution models: implications for conservation planning under climate change. Biology letters. 2009;5(1):39–43.
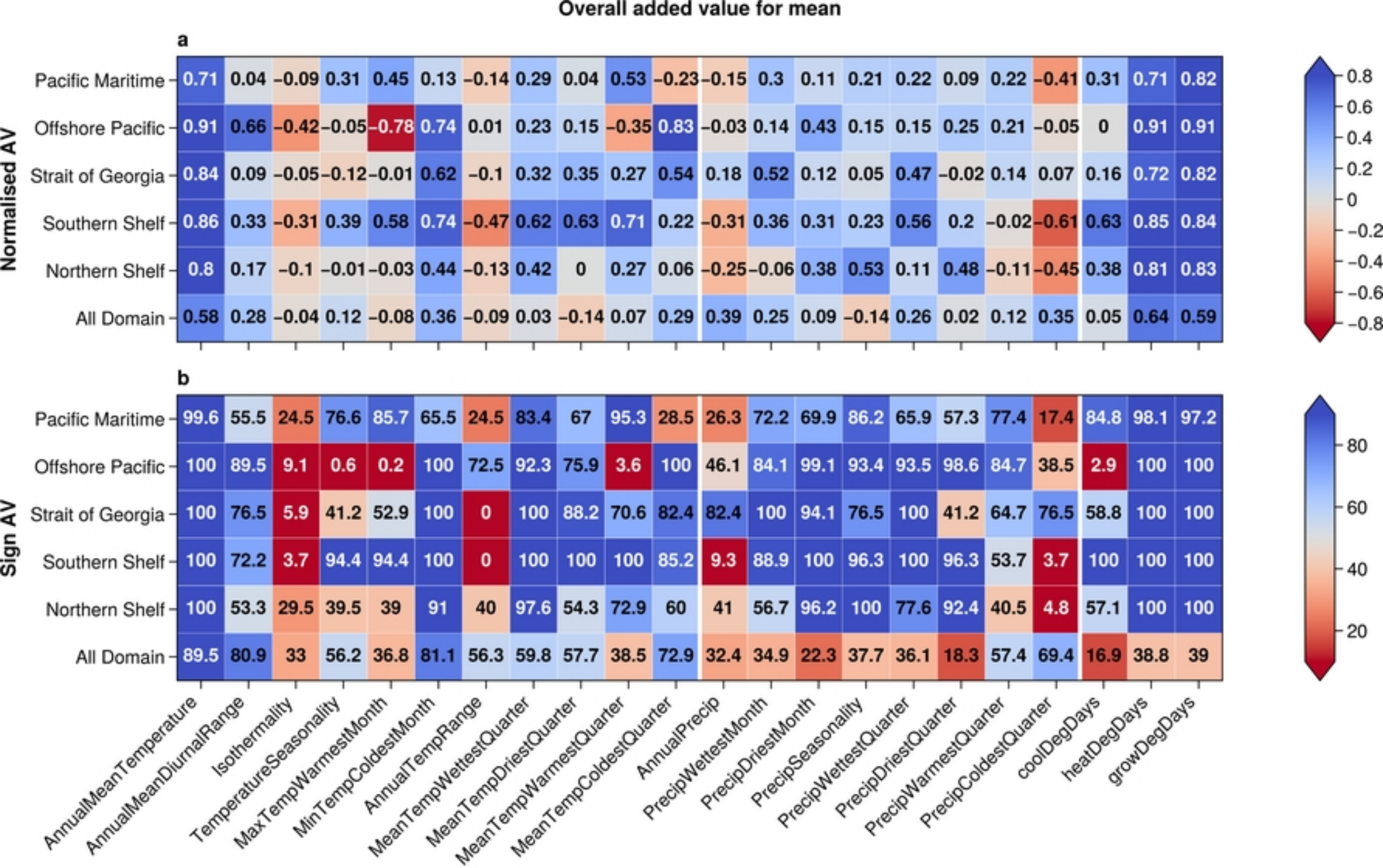
a

D1 (36km)

D2 (12km)

Model Elevation (m)

b

Northern Shelf

Offshore
Pacific
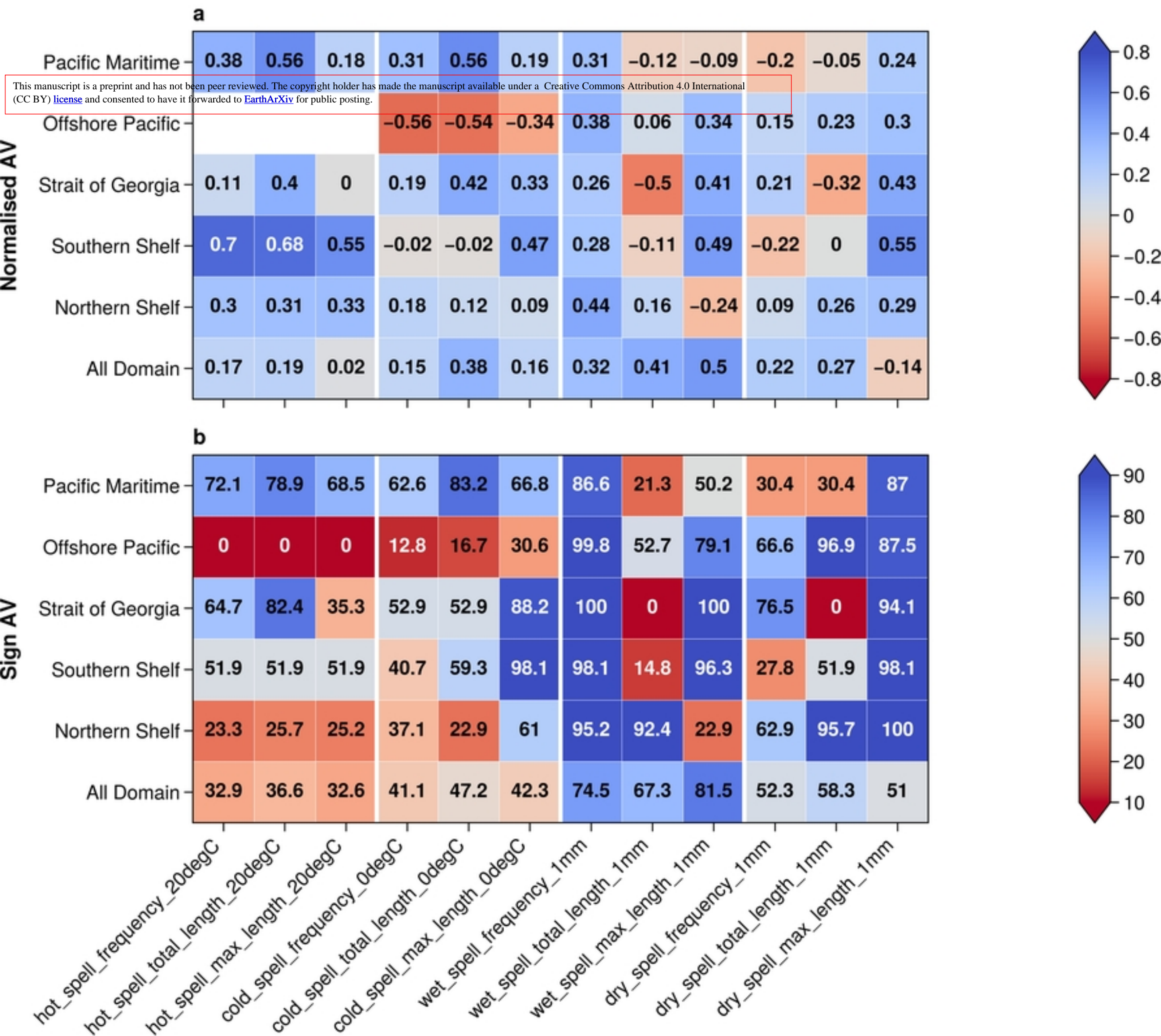
Pacific
Maritime

Southern Shelf

Strait of
Georgia

Figure

Figure

Figure

Figure

Overall added value for mean

Figure

Overall added value for mean

a

Normalised AV

	hot_spell_frequency_20degC	hot_spell_total_length_20degC	hot_spell_max_length_20degC	cold_spell_frequency_0degC	cold_spell_total_length_0degC	cold_spell_max_length_0degC	wet_spell_frequency_1mm	wet_spell_total_length_1mm	wet_spell_max_length_1mm	dry_spell_frequency_1mm	dry_spell_total_length_1mm	dry_spell_max_length_1mm
Pacific Maritime	0.38	0.56	0.18	0.31	0.56	0.19	0.31	−0.12	−0.09	−0.2	−0.05	0.24
Offshore Pacific				−0.56	−0.54	−0.34	0.38	0.06	0.34	0.15	0.23	0.3
Strait of Georgia	0.11	0.4	0	0.19	0.42	0.33	0.26	−0.5	0.41	0.21	−0.32	0.43
Southern Shelf	0.7	0.68	0.55	−0.02	−0.02	0.47	0.28	−0.11	0.49	−0.22	0	0.55
Northern Shelf	0.3	0.31	0.33	0.18	0.12	0.09	0.44	0.16	−0.24	0.09	0.26	0.29
All Domain	0.17	0.19	0.02	0.15	0.38	0.16	0.32	0.41	0.5	0.22	0.27	−0.14

b

Sign AV

	hot_spell_frequency_20degC	hot_spell_total_length_20degC	hot_spell_max_length_20degC	cold_spell_frequency_0degC	cold_spell_total_length_0degC	cold_spell_max_length_0degC	wet_spell_frequency_1mm	wet_spell_total_length_1mm	wet_spell_max_length_1mm	dry_spell_frequency_1mm	dry_spell_total_length_1mm	dry_spell_max_length_1mm
Pacific Maritime	72.1	78.9	68.5	62.6	83.2	66.8	86.6	21.3	50.2	30.4	30.4	87
Offshore Pacific	0	0	0	12.8	16.7	30.6	99.8	52.7	79.1	66.6	96.9	87.5
Strait of Georgia	64.7	82.4	35.3	52.9	52.9	88.2	100	0	100	76.5	0	94.1
Southern Shelf	51.9	51.9	51.9	40.7	59.3	98.1	98.1	14.8	96.3	27.8	51.9	98.1
Northern Shelf	23.3	25.7	25.2	37.1	22.9	61	95.2	92.4	22.9	62.9	95.7	100
All Domain	32.9	36.6	32.6	41.1	47.2	42.3	74.5	67.3	81.5	52.3	58.3	51

Figure